Contents lists available at SciOpen

Food Science and Human Wellness

journal homepage: https://www.sciopen.com/journal/2097-0765

China Food Publishing Co.

Physiological and transcriptomic insights into ethanol stress tolerance in *Lentilactobacillus hilgardii* Q19

Jinxian Sun[a,b,1], Xiaowen Liu[a,b,1], Luqiang Huang[c], Wen Ma[a,b], Gang Jin[a,b,*]

[a] *College of Enology and Horticulture, Ningxia University, Yinchuan 750021, China*
[b] *Engineering Research Center of Grape and Wine, Ministry of Education, Yinchuan 750021, China*
[c] *College of Life Science, Fujian Normal University, Fuzhou 350117, China*

ARTICLE INFO

Article history:
Received 1 May 2024
Received in revised form 19 May 2024
Accepted 19 June 2024

Keywords:
Lentilactobacillus hilgardii
Ethanol stress
Transcriptome
Gene overexpression
Molecular mechanism

ABSTRACT

Malolactic fermentation, started by lactic acid bacteria, plays a crucial role in the production of high-quality wines. As global warming increases the ethanol content in wines, the success of malolactic fermentation depends on selecting ethanol-tolerant strains, especially for wines from increasingly warm climates. *Lentilactobacillus hilgardii* Q19 was isolated and characterized as an indigenous malolactic bacterium with higher ethanol tolerance properties. In this study, it was indicated that ethanol stress had significant effects on ATPase activity, antioxidant system, and cell membrane of *L. hilgardii* Q19 by measuring the physiological indicators under stress which include H^+-ATPase, Na^+/K^+-ATPase, Ca^{2+}/Mg^{2+}-ATPase activity, glutathione content, superoxide dismutase (SOD) activity and intracellular reactive oxygen species (ROS) content. The main metabolic pathways involved in ethanol stress such as ATP-binding cassette (ABC) transporters, pentose phosphate pathway, phosphotransferase system, glutathione metabolic pathway and two-component systems were screened by transcriptome sequencing analysis. The functions of the pentose phosphate pathway, pyruvate metabolic pathway and glycerolipid metabolism under ethanol stress were verified by constructing the *L. hilgardii* Q19 ethanol stress related key genes *gntK*, *pyk*, and *glpK* overexpression vectors. The above findings may contribute to our understanding of the metabolic pathways and regulatory mechanisms of *L. hilgardii* Q19 in response to ethanol stress.

1. Introduction

Global warming has given rise to a series of consequences, including elevated temperatures, alterations in precipitation patterns, and fluctuations in solar radiation[1]. Consequently, these changes have led to noticeable variations in grape composition. Specifically, there has been an increase in sugar content and a decrease in acidity levels[2]. Alcoholic fermentation (AF) during winemaking converts the sugar in grape berries into ethanol in wines, and malolactic fermentation (MLF) initiated by lactic acid bacteria (LAB) usually follows AF[3]. This shift in grape berries has brought about a significant challenge in the form of excessive ethanol levels in wine, which poses a substantial threat to the growth of LAB during MLF[3]. The extent of cellular damage induced by ethanol primarily hinges on the concentration of ethanol that permeates the cell membrane[4]. Ethanol's toxicity as an organic solvent to LAB predominantly manifests as the disruption of cell membranes. The intrusion of ethanol into these membranes can influence the performance of crucial enzymes involved in bacterial metabolism by altering membrane structure and compromising membrane integrity[5].

In recent years, there has been a surge of interest in the development of innovative MLF strains. Recent investigations

[1] These authors contributed equally to this work.
[*] Corresponding author at: College of Enology and Horticulture, Ningxia University, Yinchuan 750021, China
E-mail address: jin.gang@nxu.edu.cn (G. Jin)
Peer review under responsibility of Beijing Academy of Food Sciences.

SciOpen Publishing services by Tsinghua University Press

http://doi.org/10.26599/FSHW.2024.9250361

have shown that *Lentilactobacillus hilgardii* is one of the novel MLF strains adapted to low-acid, high-ethanol environments. For example, *L. hilgardii* FLUB exhibited a higher resistance to elevated concentrations of ethanol (18%) and sugar (25%) compared to control strains[6]. Meanwhile, *L. hilgardii* LMG 7934 also exhibited the broader adaptive capacity than other bacterial strains[7]. *L. hilgardii* Q19 represents an indigenous LAB strain that was meticulously isolated and purified from Ningxia wine region. This strain had demonstrated remarkable resilience to adverse conditions. It was able to tolerate 19% (*V*/*V*) ethanol, which clearly exceeded the ethanol tolerance of commercial MLF starters (around 15% (*V*/*V*)). Notably, after MLF by the direct vat set starter made from *L. hilgardii* Q19 also brought wines with a richer variety and larger quantities of aromas than the commercial control, exhibiting outstanding winemaking characteristics[8]. Thus, *L. hilgardii* Q19 can be regarded as a potential candidate for the new generation of MLF starter in high alcohol wine. Based on its notable adaptation to high ethanol concentrations, *L. hilgardii* Q19 is postulated to possess unique physiological mechanisms for mitigating ethanol-induced cellular damage. However, the complex mechanism behind the *L. hilgardii* Q19 ethanol tolerance is still unknown. Therefore, clarifying the coping mechanism of *L. hilgardii* Q19 under ethanol stress is crucial to understanding the microbial response mechanisms to adversity and the construction of stress-tolerant strains.

In this study, both phenotypic and transcriptome analysis were carried out, the key metabolic pathways and corresponding genes involved ethanol stress response were mined. Initial validations of gene functionalities, shedding light on their potential contributions to ethanol tolerance were analyzed. The main metabolic pathways screened by transcriptome analysis can provide specific research directions for the stress resistance of LAB. We can also improve the efficiency of MLF under wine adversity by using genetic engineering strains. These works not only comprehensively revealed the molecular mechanism of *L. hilgardii* Q19 response to ethanol stress, but also offered an essential insight on enhancing the ethanol tolerance capabilities of LAB.

2. Materials and methods

2.1 Experimental strains and culture conditions

L. hilgardii Q19 cultivation: *L. hilgardii* Q19, an indigenous LAB strain, was isolated from Ningxia, China. This strain underwent ethanol stress treatment at concentrations of 15%, 17%, and 19% (*V*/*V*). The 19% ethanol concentration was selected for further experiments due to its high tolerance level. For cultivation, *L. hilgardii* Q19 was inoculated in MRS broth, supplemented with 20% (*V*/*V*) apple juice, and incubated at 37 °C. The viability of the bacteria was assessed using standard plate counting. The experiment was carried out in triplicate.

Escherichia coli MC1061 for plasmid cloning: *E. coli* MC1061 was employed as the cloning host for plasmid construction. Cultures of *E. coli* MC1061 were grown in Luria-Bertani (LB) broth at 37 °C.

Lactococcus lactis NZ9000 cultivation: the standard host strain, *L. lactis* NZ9000, was statically cultured in M17 broth (sourced from Qingdao Haibo, China), enriched with 0.5% glucose (GM17), at a temperature of 30 °C. Chloramphenicol was added to the medium at a concentration of 10 μg/mL.

2.2 Physicochemical index

Physicochemical indices, including H^+-ATP, Na^+/K^+-ATP, Ca^{2+}/Mg^{2+}-ATPase activity, glutathione content, superoxide (SOD) dismutase activity, and intracellular reactive oxygen species (ROS) content, along with measurements of cell membrane fluidity and cell membrane integrity, were determined and assessed by referring to the kit instructions from Solarbio (Beijing, China) and following the methodologies outlined[9-10].

2.3 Transcriptome sequencing and data analysis

Total RNA extraction from *L. hilgardii* Q19 was carried out in accordance with the manufacturer's instructions using the RNA prep Pure Total RNA extraction kit (DP430, Tengen, Beijing, China). Two distinct groups including, the control group, consisting of *L. hilgardii* Q19 grown under no ethanol stress conditions, and the test group, comprising *L. hilgardii* Q19 cultivated under 19% (*V*/*V*) ethanol stress conditions were studies. Samples were collected during the logarithmic growth phase at 24 h, and bacterial bodies were harvested. Each treatment consisted of 3 independent biological replicates. Subsequently, the test samples were submitted to Novozymes (Beijing, China) for transcriptome sequencing and further data analysis.

2.4 Construction of overexpression vectors and functional verification of the key genes

2.4.1 Construction of overexpression vector

L. hilgardii Q19 DNA was extracted using the bacterial genomic DNA rapid extraction kit (Bacterial Genomic DNA Isolation Kit, Generay Biotech Co. Ltd., Shanghai, China). *L. hilgardii* Q19 DNA was used as a template, Primer Premier 5.0 was used to design the primers. Full-length target genes were amplified using PCR (Tables 1 and 2). Gel extraction kit D2500 (Omega Bio-Tek, Guangzhou, China) was used to extract and purify the cut bands. The isolated genes were then transformed to pNZ8148 plasmid (Miaoling Biology, Wuhan, China), cloned into the MC1061 high-efficiency competent cells and cultured on ampicillin (50 μg/mL) containing LB medium. Three colonies were chosen based on the electrophoresis profile of colony PCR products using gene specific pair of primers (Table 3) and sequenced by Shanghai Sangon Bio-Tech (Shanghai, China).

Table 1
Target gene full-length amplification system.

Reagents	Volume (μL)
HiFi TransTaq DNA Polymerase	0.5
HiFi TransTaq DNA Polymerase buffer	5.0
dNTPs	2.0
Forward Primer	0.5
Reverse Primer	0.5
DNA	1.0
ddH_2O	15.5

Table 2
Reaction conditions of PCR amplification.

Point	Cycle number	Temperature	Time
Initial Denaturation	1	94 ℃	5 min
Denaturation		94 ℃	30 s
Annealing	30	*pyk* 52 ℃/*gntK* 53.7 ℃/*glpK* 48 ℃	30 s
Extension		72 ℃	30 s
Extension	1	72 ℃	7 min

Table 3
Primers of target gene.

Name	Primer Sequence（5′−3′）	Length
pyk	F: cactcaccatgggtactgcag ATGAAGAAAACTAAGATCGTAAGTACATTG R: agtggtaccgcatgcctgcag TTATAGTGAGCTTGAAGCACCGTG	1 815 bp
gntK	F: cactcaccatgggtactgcag GGTGTATTTTCAGATTCGAAAACCG R: agtggtaccgcatgcctgcag TTATTTCCCCGAGAAATCATCTTC	1 650 bp
glpK	F: cactcaccatgggtactgcag ATGCTTACTGATAGACCAAAATATGTACTT R: agtggtaccgcatgcctgcag TTAAATCTTTGTTAATTTATATGCCCTTG	1 545 bp

Note: Lowercase portion is the homology arm of plasmid pNZ8148, underlined portion is the *pstI* cleavage site, and uppercase portion is the primer for the target gene.

The single enzyme digestion reaction system (Table 4) was introduced into 0.2 mL PCR tubes and thoroughly blended. Subsequently, enzyme digestion was executed at 37 °C for a duration of 4 h. Following the completion of enzyme digestion, the reaction mixtures were subjected to agarose gel electrophoresis. The linearized plasmid was then isolated using a gel recovery kit and subsequently stored at –20 °C for future use.

Table 4
Single enzyme digestion reaction system of pNZ8148.

Reagents	Amount
DNA	1.0 μg
10 × CutSmart	5.0 μL
PstI-HF	1.0 μL
ddH_2O	to 50 μL

Single colonies grown on LB solid plates containing 10 μg/mL chloramphenicol were individually collected and dissolved in 100 μL of sterile water. All isolated single colonies underwent colony PCR to initially confirm their status as positive clones. The colony PCR system followed the specifications outlined in Table 5, and the amplification reaction conditions were referenced from Table 2. The positive clone strain harboring the target gene was streaked onto chloramphenicol resistance plates containing 25 μg/mL chloramphenicol. Single colonies were picked for overnight incubation at 37 °C, followed by plasmid extraction and digestion with the *pstI* restriction endonuclease for 30 min at 37 °C, as detailed in Tables 4 and 6. Finally, the positively sequenced clones were mixed with a bacterial solution in a 1:1 ratio with 50% glycerol and stored at –80 °C for future use.

Positive clone strains with confirmed sequencing results were selected for plasmids pNZ8148, pNZ8148-*pyk*, pNZ8148-*gntK*, and pNZ8148-*glpK*. *L. lactis* NZ9000 culture, stored at –80 °C, was thawed on ice. Subsequently, 100 μL of bacterial solution was evenly spread onto GM17 solid plates containing varying concentrations of chloramphenicol (5, 10, 20 μg/mL), as well as plates with no chloramphenicol, and incubated in an inverted position at 30 °C overnight.

Table 5
Colony PCR amplification system.

Reagents	Volume (μL)
HiFi Trans*Taq* DNA Polymerase	0.5
HiFi Trans*Taq* DNA Polymerase buffer	5.0
dNTPs	2.0
Forward Primer	0.5
Reverse Primer	0.5
DNA	1.0
ddH_2O	15.5

Table 6
Connection system between target gene and linearized pNZ8148.

Reagents	Amount
pNZ8148 fragment	150 ng
Target gene fragment	75 ng
5 × buffer	4 μL
NovoRec® Plus diastase	1 μL
ddH_2O	add to 20 μL

2.4.2 Nisin induces protein expression of key genes in L. lactis NZ9000

The positive clones were cultured in 100 mL GM17 medium supplemented with 10 μg/mL chloramphenicol at a 2% (*V*/*V*) inoculum concentration following GM17 activation. Cultures were incubated at 30 °C, and the optical density at 600 nm ($OD_{600\ nm}$) was monitored at 30 min intervals. Upon reaching an $OD_{600\ nm}$ of approximately 0.3–0.4, 10 μL of Nisin at a concentration of 50 μg/mL was added to induce protein expression, and a growth curve was subsequently plotted.

For *L. lactis* NZ9000-pNZ8148, *L. lactis* NZ9000-pNZ8148/*gntK*, *L. lactis* NZ9000-pNZ8148/*pyk*, and *L. lactis* NZ9000-pNZ8148/*glpK* strains, cultures were prepared, and 50 mL of bacterial solution was collected for Nisin-induced target gene expression. Bacterial bodies were harvested *via* centrifugation at 5 000 × *g* and 4 °C for 10 min. The bacterial pellets were resuspended in 1 × PBS solution, supplemented with 3 mg/mL lysozyme, and maintained at 37 °C for 30 min, with intermittent shaking to ensure thorough contact between the lysozyme and bacteria. Following the incubation period, bacterial cells were subjected to ultrasonication using an ultrasonic crusher under the following conditions: 300 W power, 5 s ultrasonication, 5 s pause, and a total duration of 30 min. After ultrasonication, bacteria were collected by centrifugation at 5 000 × *g* and 4 °C for 10 min. The resulting supernatant represented the crude extract. Protein content was quantified, and 10× loading buffer was added before boiling for 5 min and freezing at –20 °C. Subsequently, the samples were undergoing SDS-PAGE. After electrophoresis, the separator gel was stained with Thomas Brilliant Blue (Beyotime Biotechnology, Shanghai, China) rapid staining solution and subsequently decolorized using distilled water. Bands were observed to confirm induced protein expression.

2.4.3 Gene functional analysis under ethanol stress

For the positive clone strain, a 50 mL culture was inoculated at a 2% (*V*/*V*) inoculum concentration after GM17 activation and incubated at 30 °C until reaching an $OD_{600\ nm}$ of approximately 0.3–0.4. Protein expression was induced by adding 5 μL of 50 μg/mL Nisin. After an additional incubation for 3 h, cells were transferred to 10 mL of GM17 liquid medium containing 10 μg/mL chloramphenicol, 1 μL of 50 μg/mL Nisin inducer, and various concentrations of anhydrous ethanol (4%, 8%, 10%, 12%, and 14% (*V*/*V*)) at a 2% (*V*/*V*) inoculum size. Cell survival was determined after 3 h of exposure to the ethanol stress. The viability of the bacteria was assessed by using standard plate counting, and was calculated as equation (1). The experiment was carried out in triplicate.

$$\text{Survival rate (\%)} = \frac{\text{Number of viable bacteria under ethanol – free stress}}{\text{Number of viable bacteria under ethanol stress}} \times 100 \quad (1)$$

3. Results and discussion

3.1 Physical and chemical indicators analysis

3.1.1 Growth curve of *L. hilgardii* Q19 under ethanol stress

L. hilgardii Q19 was inoculated into MRS medium containing different concentrations of ethanol, and the viable cell count was determined during 0–120 h. As shown in Fig. 1, *L. hilgardii* Q19 started to enter the logarithmic phase at 3 h under no ethanol stress, with the fastest growth rate at 24 h. The viable cell counts reached the maximum and the stationary phase was reached at 120 h. Under 15% and 17% (*V*/*V*) ethanol stress, *L. hilgardii* Q19 showed a certain degree of decrease in viable counts at 3 h. Since 24 h, the strains gradually adapted to the stress environment. The viable cell counts increased steadily and reached the maximum value at 120 h. Under 19% (*V*/*V*) stress, the number of *L. hilgardii* Q19 decreased significantly at 24 h but remained stable after 48 h, indicating that *L. hilgardii* Q19 has a response mechanism to cope with ethanol stress.

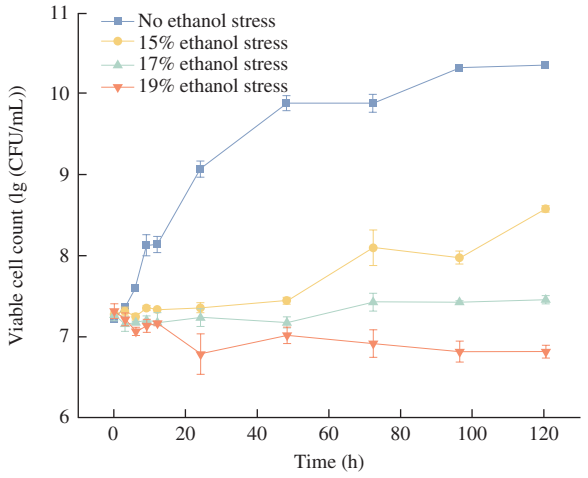

Fig. 1 Growth curve of *L. hilgardii* Q19 under ethanol stress.

3.1.2 Cell membrane permeability

As shown in Fig. 2A, ethanol had a significant effect on the H^+-ATPase activity of *L. hilgardii* Q19. Compared to the control group, the activity of H^+-ATPase under 19% (*V*/*V*) ethanol exhibited a significant reduction of 71.0%, 75.2%, and 65.9% during different growth periods (3, 24, and 120 h, respectively). H^+-ATPase plays an important role in maintaining cellular homeostasis and aiding transport of substances across membranes under stress conditions[11]. Some authors who have worked with LAB have shown that the intracellular H^+-ATPase activity is usually decreased under stress[12-14].

Furthermore, Na^+/K^+-ATPase activity exhibited significant differences ($P < 0.05$) between the 19% (*V*/*V*) ethanol stress and the no-stress environment at both 3 and 24 h (Fig. 2B). Specifically, Na^+/K^+-ATPase activities decreased by 46.3% and 37.1% under stress conditions compared to their unstressed counterparts, respectively. The activity of Na^+/K^+-ATPase of *L. hilgardii* Q19 was decreased under ethanol stress and Na^+/K^+ ion transport was affected. The osmotic pressure inside and outside the cell membrane is altered, causing cellular damage. It also affects the coupling of ATP to ADP, which influences strain survival by altering intracellular ATP supply. Although the control group was lower than the experimental group at 120 h, the data were not significantly different. Under 19% (*V*/*V*) ethanol stress, the activity of Ca^{2+}/Mg^{2+}-ATPase slightly increased by 0.05% after 3 h, but decreased by 0.06% and 0.24% after 24 h and 120 h, respectively (Fig. 2C). These changes were not statistically significant when compared to the stress-free environment, so ethanol stress may not have affected the exchange of Ca^{2+} and Mg^{2+} ions.

Collectively, these results underscore the susceptibility of H^+-ATPase and Na^+/K^+-ATPase activity to ethanol-induced toxicity, leading to a reduction in enzyme activity. This reduction subsequently impacts the transport of Na^+ and K^+ ions across the cell membrane, influencing osmotic pressure dynamics within and outside the cell membrane[11,15]. Consequently, these alterations contribute to cellular damage and inhibition of bacterial growth.

3.1.3 Antioxidant system

SOD enzyme activity was slightly reduced under ethanol stress conditions at 3 and 24 h (Fig. 2D). However, SOD activity decreased more during the growth stabilization period (120 h), indicating a more pronounced impact on SOD enzyme activity in prolonged ethanol stress conditions. Several studies have indicated that enhancing SOD expression is an effective method to increase cell survival rate under H_2O_2 stress[16-17]. However, there are relatively few studies on SOD enzyme activity under ethanol stress. In our case, the change in SOD enzyme activity was not significant, so SOD may not serve as the primary pathway for oxygen radical scavenging in the ethanol stress environment.

Glutathione is a non-protein thiol compound which can protect probiotics from different stresses[18-20]. The analysis of intracellular glutathione content revealed the highest levels of glutathione content were observed in both groups of *L. hilgardii* Q19 samples at the 24-h mark (Fig. 2E). Additionally, after 3, 24, and 120 h of ethanol stress, the intracellular glutathione content was

significantly elevated, reaching 3.76, 5.26, and 5.04 times of the control group, respectively. However, it is important to note that the glutathione content remained relatively low in both the experimental and control groups. This is primarily attributed to the fact that some LAB lack the inherent ability to synthesize glutathione independently and rely on external sources for its acquisition[21]. Uptaking glutathione can enhance the resistance of LAB under stress conditions[22-23]. For instance, during wine fermentation, the addition of glutathione can help LAB adapt to the adversity of high ethanol concentration[23]. At the same time, glutathione can also regulate the color and flavor of the wine[24].

In general, low concentrations of ROS play a regulatory role in cellular functions, while excessive ROS can lead to oxidative stress-induced damage to various biomolecules such as proteins, lipids, and nucleic acids[25-26]. The detection of 2′,7′-dichlorofluorescein (DCF) fluorescence can serve as an indicator of intracellular ROS levels, with higher fluorescence intensity corresponding to elevated ROS levels[27]. The results presented in Fig. 2F demonstrate that, across all 3 time periods, the fluorescence intensity of cells subjected to 19% (*V*/*V*) ethanol stress conditions was significantly lower than that of the control group. This suggests that under stress conditions, the intracellular ROS content was lower. This observed phenomenon may be attributed to ethanol stress prompting increased cellular uptake of glutathione from the external environment[22]. Glutathione serves as a reducing agent that scavenges a portion of oxygen radicals, thereby reducing intracellular ROS content[28]. Notably, the lower fluorescence intensity observed at 3 and 24 h, compared to the 120-h time point, may be attributed to a decline in cellular metabolic capacity during the late stage of strain growth. This reduced capacity could lead to weakened extracellular substance exchange and the subsequent accumulation of intracellular ROS, resulting in elevated fluorescence intensity[25-26].

3.1.4 Cell membrane fluidity

In the evaluation of cell membrane fluidity using DPH[29], it was observed that fluorescence intensity significantly decreased under stress conditions, indicating a reduction in cell membrane fluidity (Fig. 2G). In agreement with our findings, multiple studies have shown that LAB can reduce cell damage by decreasing cell membrane fluidity[30-31]. However, stress conditions can also increase the membrane fluidity of LAB[32-33]. This suggests that the alteration of cell membrane fluidity in stressful environments is specific to different strains. Remarkably, the difference in fluorescence intensity between the 3 time periods was not statistically significant under ethanol stress. This suggests that the impact on cell membrane fluidity commenced early in the stress induction and persisted throughout the experiment. This alteration in cell membrane fluidity appears to be a rapid adaptive response triggered as cells enter the stress environment, indicative of an ongoing coping mechanism against ethanol stress[32,34].

3.1.5 Cell membrane integrity

The integrity of the cell membrane, as the first line of defense of microorganisms against adverse environments, directly affects cellular resistance[35]. Propidium iodide (PI) is a fluorescent molecule that binds to nucleic acids in cells to produce red fluorescence[36]. Higher fluorescence intensity indicates more serious cell membrane damage. As depicted in Fig. 2H, the fluorescence intensity of cells exposed to the ethanol stress environment consistently lower than that of the control group throughout the experiment. There were no statistically significant differences in fluorescence intensity between the experimental group and the control group at both 3 and 120 h ($P < 0.05$). In contrast, at the 24-h time point, the fluorescence intensity of the experimental group was significantly lower than that of the control group. During this phase, ethanol stress may have a notable impact on the cell membrane structure and thus may affect its function. This effect can be attributed to the relatively high rate of cell metabolism and the frequent exchange of substances both within and outside the cell during logarithmic growth period[37]. This result is consistent with the study of *Tetragenococcus halophilus* under ethanol stress[38]. After ethanol stress, cell shrinkage, volume reduction, and breakdown of cell membrane integrity were occurred in the cells.

Physical and chemical indicators analysis of *L. hilgardii* Q19 showed that the cell membrane fluidity was reduced and the ability to exchange substances decreased under the stress environment. This is a common feature of most LAB in response to environmental stress[30-31]. Meanwhile, ethanol stress significantly increased cellular Glutathione uptake, scavenged of intracellular ROS, and reduced oxidative damage to the cells. This may be the main reason why *L. hilgardii* Q19 has a good ability to cope with 19% (*V*/*V*) ethanol stress.

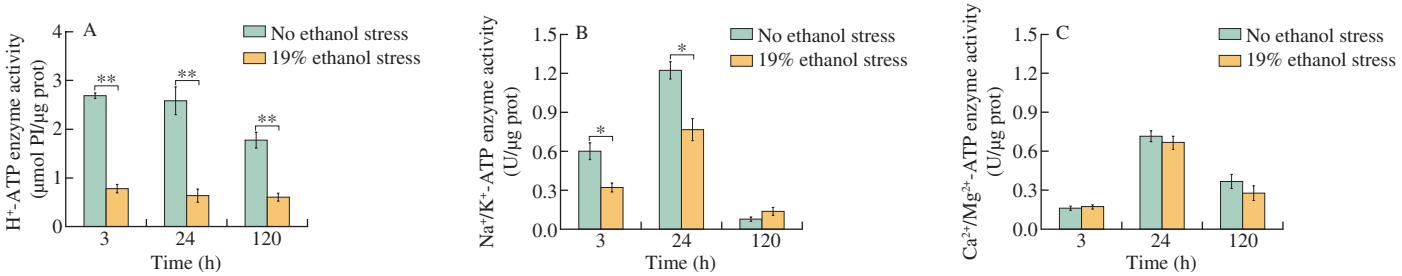

Fig. 2 (A) H^+-ATPase activity of *L. hilgardii* Q19 under ethanol stress. (B) Na^+/K^+-ATPase activity of *L. hilgardii* Q19 under ethanol stress. (C) Ca^{2+}/Mg^{2+}-ATPase activity of *L. hilgardii* Q19 under ethanol stress. (D) SOD activity of *L. hilgardii* Q19 under ethanol stress. (E) Intracellular glutathione content of *L. hilgardii* Q19 under ethanol stress. (F) Intracellular ROS of *L. hilgardii* Q19 under ethanol stress. (G) Cell membrane fluidity of *L. hilgardii* Q19 under ethanol stress. (H) Cell membrane integrity of *L. hilgardii* Q19 under ethanol stress. $^*P < 0.05$, $^{**}P < 0.01$.

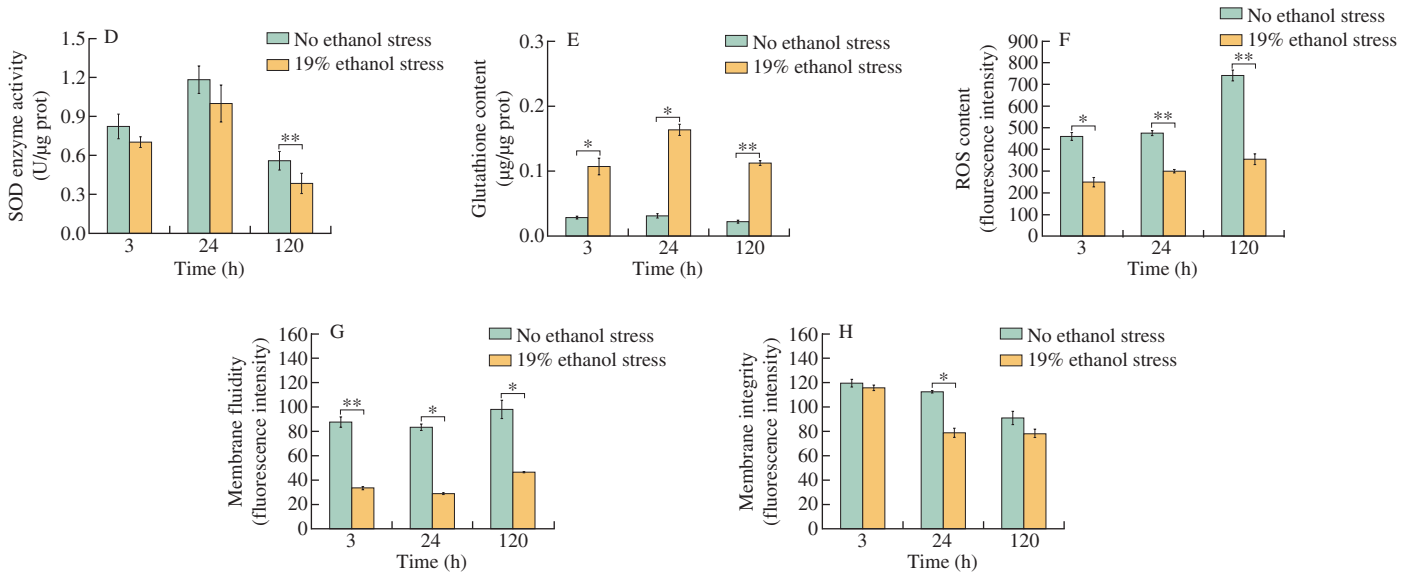

Fig. 2 (*Continued*)

3.2 Differential expression analysis of key metabolic pathways

3.2.1 Gene ontology (GO) annotation analysis of differentially expressed genes

The transcriptome data showed that 1 347 genes were differentially expressed in *L. hilgardii* Q19 under 19% ethanol stress compared to no stress, of which 680 genes were up-regulated and 667 genes were down-regulated (Fig. 3). The up-regulated differentially expressed genes showed a significant enrichment (Fig. 4A), mainly in the structural composition of ribosomes, ribonucleoprotein complex, cellular protein metabolism process, protein metabolism process and amide biosynthesis process. The down-regulated differential genes were mainly in galactosidase activity, structural composition of the cytoskeleton, carbohydrate metabolism process and protein-lipid complexes (Fig. 4B).

3.2.2 KEGG analysis of differentially expressed genes

Multiple aspects of *L. hilgardii* Q19 change together in response to ethanol stress, rather than being simply regulated by a single gene. The main KEGG pathways shown in Fig. 5 are ABC transporter (Ibr02010), pentose phosphate pathway (Ibr00030), two-component system (02020), arginine and proline metabolism (00330), glutathione metabolism (00480), pyruvate metabolism (Ibr00620).

3.2.2.1 Changes in ABC transporters metabolic pathway

The superfamily of ABC transporter proteins is ubiquitous across all domains of life, playing a pivotal role in a myriad of biological processes. These proteins utilize ATP to translocate a diverse array of substrates, ranging from ions to proteins, across cellular membranes[39]. ABC transporter proteins are instrumental in bacterial survival and adaptation

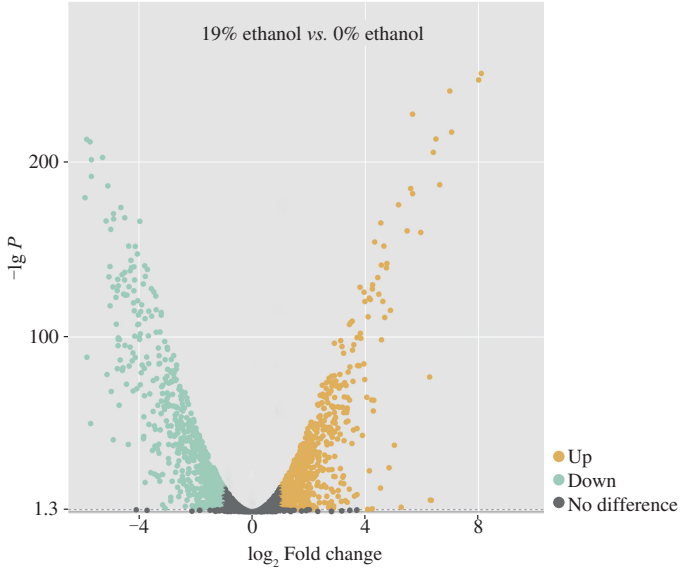

Fig. 3 Volcano plots of the gene expression profile in Q19-19% ethanol *vs*. Q19-0% ethanol.

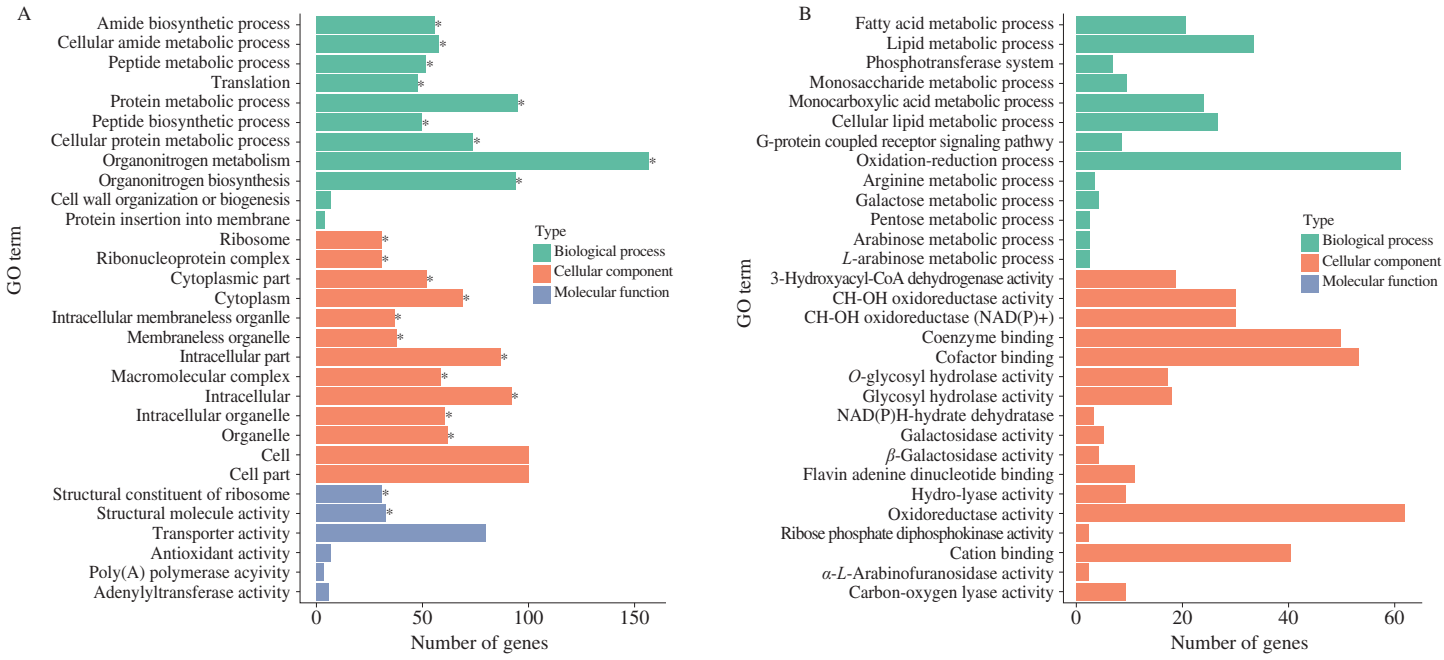

Fig. 4 GO enrichment analysis of differentially expressed genes. The ordinate is the enrichment of the GO term, and the horizontal axis is the number of different genes in the term. (A) Up-regulated expressed genes; (B) down-regulated expressed genes.

under different environmental stress[40-44]. In the ABC transporters metabolic pathway (Table 7), *pstB* (GQR93_RS14410), *pstA* (GQR93_RS09185), *pstS* (GQR93_RS14425) and *pstC* (GQR93_RS09190) were significantly down-regulated under 19% (*V*/*V*) ethanol stress. PstB is the ATP-binding component and PstA/PstC are two hydrophobic subunits of phosphate permease belonging to the ABC transporter protein family[45-46]. They bind ATP to release energy and participate in carbon metabolism, nitrogen metabolism to maintain cellular homeostasis[47]. The down-regulation of *pst* genes may be due to the slower metabolism of *L. hilgardii* Q19 under ethanol stress condition.

3.2.2.2 *Changes in pentose phosphate pathway*

In the pentose phosphate pathway (Table 8), a notable decrease was observedin the transcription of *gntK* (GQR93_RS10480) and *gndA* (GQR93_RS13035), which are involved in gluconate transport and phosphorylation and encoding of primary 6-phosphate-gluconate dehydrogenase, respectively. Conversely, *eda* (GQR93_RS13035), associated with the ED pathway, are increased. This upregulation indicates the shortest route to synthesizing pyruvate from gluconate is active[48]. Ribulose-5-phosphate isomerase A (RpiA) is a key enzyme

Table 7
ABC transporters metabolic pathway gene expression changes.

Gene number	Relative expression	Gene name	Description of gene function
GQR93_RS03110	1.125 1	–	Iron ABC transporter permease
GQR93_RS11340	–1.18	–	Amino acid ABC transporter ATP-binding protein
GQR93_RS11685	3.673 2	–	Spermidine/putrescine ABC transporter substrate-binding protein
GQR93_RS00210	1.421 8	–	Carbohydrate ABC transporter permease
GQR93_RS14410	–3.192 2	*pstB*	Phosphate ABC transporter ATP-binding protein
GQR93_RS10600	2.784	–	Proline/glycine betaine ABC transporter permease
GQR93_RS10605	2.311	–	Glycine betaine/*L*-proline ABC transporter ATP-binding protein
GQR93_RS09185	–2.634 1	*pstA*	Phosphate ABC transporter permease PstA
GQR93_RS10265	1.327 6	*cydD*	Thiol reductant ABC exporter subunit CydD
GQR93_RS03105	1.007 2	–	Iron chelate uptake ABC transporter family permease subunit
GQR93_RS07320	3.566 7	–	ABC transporter permease
GQR93_RS02325	–1.334 5	*sufC*	Fe-S cluster assembly ATPase SufC
GQR93_RS00610	2.346 5	–	Amino acid ABC transporter permease
GQR93_RS14425	–2.586 2	*pstS*	Phosphate ABC transporter substrate-binding protein PstS family protein
GQR93_RS11675	1.048 8	*potA*	ABC transporter ATP-binding protein
GQR93_RS08755	–3.913 9	–	Peptide ABC transporter substrate-binding protein
GQR93_RS04300	1.784 3	–	ABC transporter permease/substrate-binding protein
GQR93_RS12085	–4.193 5	–	Energy-coupling factor transporter transmembrane protein EcfT
GQR93_RS12080	–4.151 8	–	ATP-binding cassette domain-containing protein
GQR93_RS11820	2.187 7	–	Transporter substrate-binding domain-containing protein
GQR93_RS09190	–2.415 3	*pstC*	Phosphate ABC transporter permease subunit PstC

Note: "–" indicates gene not yet named.

facilitating the conversion between ribulose-5-phosphate and ribose-5-phosphate, pivotal in both the pentose phosphate pathway and the Calvin cycle[49]. Its function allows to produce ribose from various sugars and the salvage of sugars from ribonucleotide breakdown[50]. The pentose phosphate pathway is a crucial regulator of cellular reductive-oxidative (redox) balance and biosynthesis, traditionally recognized for supplying reducing power and ribose phosphate[49]. An increase in *rpiA* (GQR93_RS13505) and *gnd* (GQR93_RS12865) transcription signifies an active pentose phosphate pathway, suggesting that under stress conditions, the strain adapts by boosting NADPH production to maintain its energy metabolism.

3.2.2.3 Changes in two-component system pathway

The two-component system is a vital signaling mechanism present in both Gram-positive/negative bacteria, governing a range of physiological responses and metabolic processes[51]. In the two-component system pathway (Table 9), the gene GQR93_RS12910, which encodes HAMP domain-containing histidine kinase, was significantly up-regulated. The gene *maeA* (GQR93_RS14055), encoding NAD-dependent malic enzyme, was also up-regulated. In previous studies, genes regulating the two-component system are usually up-regulated under ethanol stress[52]. Meanwhile, Two-component system plays an important role in bacterial adaptation to adversity, including acid and oxidative tolerance[53-54]. It is believed that the diversity of two-component systems enhances bacterial survival and adaptation across different habitats[55]. Two-component system is a part of the bacterial quorum sensing (QS) apparatus[56]. The QS system protects the LAB from stresses by regulating biofilm formation[57-58].

3.2.2.4 Changes in arginine and proline metabolic pathway

When LAB is exposed to abiotic stresses, the arginine deiminase (ADI) pathway is an important mechanism in response to stress[59-61]. Arginine is degraded to CO_2, ornithine and ammonia mainly by ADI, ornithine carbamoyltransferase (OTC) and carbamate kinase (CK)[62]. The response of *arcA*, *arcB*, and *arcC*, which encode ADI, OTC, and CK, respectively, was demonstrated under ethanol stress[61]. The presence of these three genes was confirmed in *Oenococcus oeni* and *L. hilgardii*, suggesting that the ADI pathway can respond to stress[63]. In the arginine and proline pathway (Table 10), *arcC* and *aguA* decreased significantly.

3.2.2.5 Changes in glutathione metabolism pathway

Glutathione biosynthesis commences with the formation of a peptide bond between glutamate and cysteine, a reaction catalyzed by γ-glutamylcysteine synthetase (GshA)[64]. This step is followed by the bonding of γ-Glu-Cys to glycine, facilitated by glutathione synthetase (GshB). Within glutathione metabolism, glutathione peroxidase and glutathione reductase are key enzymes. The former catalyzes the oxidation of glutathione to glutathione disulfide (GSSG), while the latter restores glutathione from its oxidized state[65]. In a study by Margalef-Català et al.[23] cells cultured with glutathione showed higher survival rate when exposed to ethanol shock at a concentration of 4% (*V*/*V*). Analysis of transcriptomic data has revealed that genes involved in the glutathione metabolic pathway are consistently up-regulated (Table 11), suggesting an elevated glutathione uptake in response to ethanol stress. Enhancing the ability to take up glutathione can help *L. hilgardii* Q19 to better cope with ethanol stress.

3.2.2.6 Changes in pyruvate metabolic pathway

Pyruvate kinase plays a crucial role in cellular metabolism by catalyzing the transfer of a phosphate group from phosphoenolpyruvate to ADP, thereby producing ATP and pyruvate[66]. Pyruvate itself

Table 8
Pentose phosphate pathway gene expression changes.

Gene number	Relative expression	Gene name	Description of gene function
GQR93_RS10480	–2.510 9	*gntK*	Gluconokinase
GQR93_RS13035	–2.756 2	*gndA*	NADP-dependent phosphogluconate dehydrogenase
GQR93_RS13030	1.119 9	–	Glucose-6-phosphate dehydrogenase
GQR93_RS13505	3.534 2	*rpiA*	Ribose-5-phosphate isomerase RpiA
GQR93_RS05010	1.570 5	*eda*	Bifunctional 4-hydroxy-2-oxoglutarate aldolase/2-dehydro-3-deoxy-phosphogluconate aldolase
GQR93_RS10590	–4.740 5	*deoC*	Deoxyribose-phosphate aldolase
GQR93_RS12225	–2.248 7	–	Lactonase family protein
GQR93_RS10585	–4.504 3	–	Phosphopentomutase
GQR93_RS05805	–1.103 4	*rbsK*	Ribokinase
GQR93_RS12865	1.197 9	gnd	Decarboxylating 6-phosphogluconate dehydrogenase
GQR93_RS10155	–1.134 6	–	Ribose-phosphate diphosphokinase

Note: "–" indicates gene not yet named.

Table 9
Two-component system gene expression changes.

Gene number	Relative expression	Gene name	Description of gene function
GQR93_RS14055	1.613 3	*maeA*	NAD-dependent malic enzyme
GQR93_RS01355	–1.791 6	–	Sensor histidine kinase
GQR93_RS00005	1.568	*dnaA*	Chromosomal replication initiator protein DnaA
GQR93_RS12910	4.444 6	–	HAMP domain-containing histidine kinase
GQR93_RS10275	–1.513	–	Cytochrome ubiquinol oxidase subunit I
GQR93_RS10270	–1.516 9	*cydB*	Cytochrome d ubiquinol oxidase subunit II

Note: "–" indicates gene not yet named.

serves as a key juncture for numerous metabolic pathways. Analysis of transcriptome data reveals that *pyk* (GQR93_RS07430), *adhE* (GQR93_RS12980) and *maeA* (GQR93_RS14055) involved in the pyruvate metabolic pathway are up-regulated (Table 12), indicating enhanced efficiency of pyruvate metabolism in environments abundant in glucose and other sugars. The *adhE* gene has been linked to the thermal tolerance of LAB. The expression of this gene has led to significant improvements in survival, cellular hydrophobicity, and membrane integrity at elevated temperatures[67].

The key gene changes in different pathways suggest that multiple aspects of *L. hilgardii* Q19 act together in response to ethanol stress rather than a simple stress response regulated by a single gene. The ABC transporters play an important role in ion exchange and cell membrane production. At the same time, the pentose phosphate

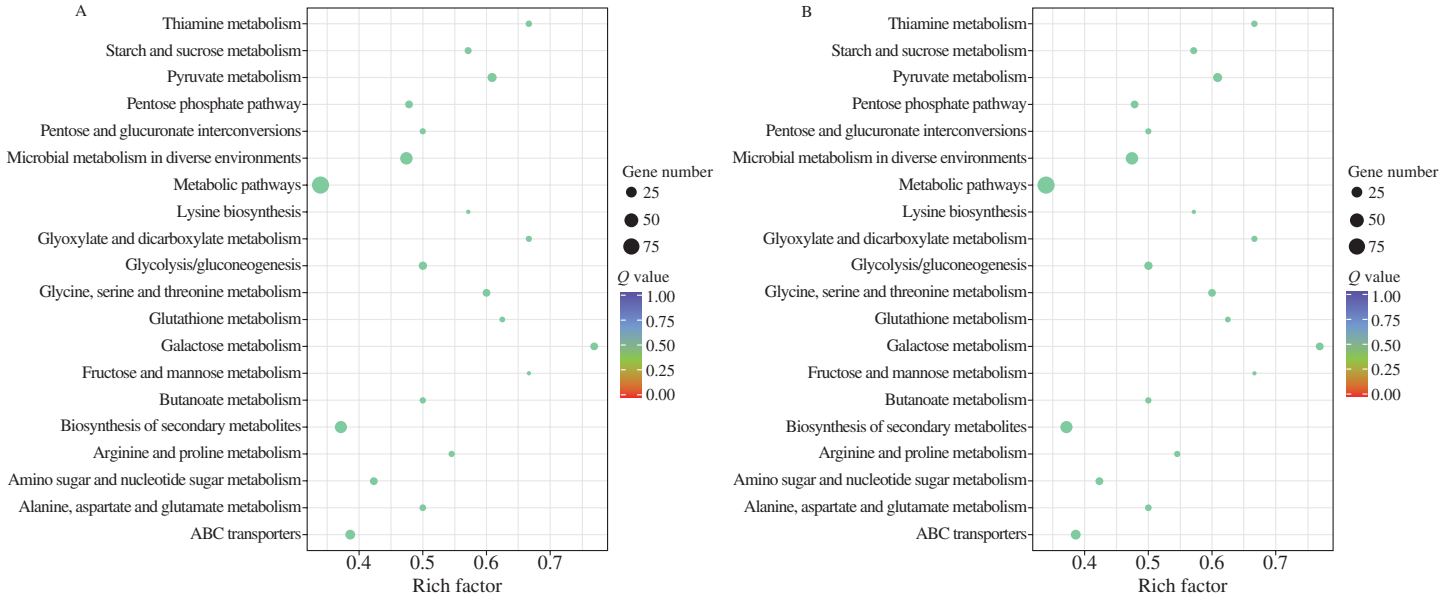

Fig. 5 KEGG enrichment analysis results. (A) Up-regulated expressed genes; (B) down-regulated expressed genes.

Table 10
Arginine and proline metabolism pathway gene expression changes.

Gene number	Relative expression	Gene name	Description of gene function
GQR93_RS01340	–1.041 1	*arcC*	Carbamate kinase
GQR93_RS12390	–1.193 5	*codA*	Cytosine deaminase
GQR93_RS11805	–4.180 2	–	Pseudogene
GQR93_RS11405	2.024 9	–	Proline-specific peptidase family protein
GQR93_RS01375	–1.638 7	*aguA*	Agmatine deiminase

Note: "–" indicates gene not yet named.

Table 11
Glutathione metabolic pathway gene expression changes.

Gene number	Relative expression	Gene name	Description of gene function
GQR93_RS01190	1.357 8	–	Glutathione peroxidase
GQR93_RS05540	1.365 6	–	γ-Glutamylcysteine synthetase
GQR93_RS12865	1.197 9	*gnd*	Decarboxylating 6-phosphogluconate dehydrogenase
GQR93_RS13030	1.119 9	–	Glucose-6-phosphate dehydrogenase

Note: "–" indicates gene not yet named.

Table 12
Pyruvate metabolic pathway gene expression changes.

Gene number	Relative expression	Gene name	Description of gene function
GQR93_RS04365	1.108 6	–	*L*-Lactate dehydrogenase
GQR93_RS06360	3.319 2	–	Pyruvate oxidase
GQR93_RS07430	1.311 2	*pyk*	Pyruvate kinase
GQR93_RS08460	1.048 5	–	Acylphosphatase
GQR93_RS12490	1.983 77	*ilvB*	Biosynthetictype acetolactate synthase large subunit
GQR93_RS12980	5.485 5	*adhE*	Bifunctional acetaldehyde-CoA/alcohol dehydrogenase
GQR93_RS13110	2.757 9	–	Thiolase family protein
GQR93_RS14055	1.613 3	*maeA*	NAD-dependent malic enzyme

Note: "–" indicates gene not yet named.

pathway and pyruvate metabolism, which supply energy to the cell, were also significantly affected. Therefore, down-regulation of ion exchange and carbon source metabolism genes reduced cell membrane fluidity and the ability to exchange substances under stress. *L*-Glutamate, a metabolite in arginine and proline metabolism, also can direct participate in many other pathways (e.g. glutathione metabolism). The uptake glutathione ability of *L. hilgardii* Q19 was enhanced in response to ethanol stress through up-regulating genes in the glutathione metabolic pathway. In addition, the activities of H^+-ATPase, Na^+/K^+-ATPase, Ca^{2+}/Mg^{2+}-ATPase were affected by down-regulating genes related to cation-transporting P-type ATPase (Table 13).

3.3 Functional validation of key genes

Ethanol stress, as an abiotic stress, causes changes in a variety of physiological responses in microorganisms, mainly including sugar metabolism, lipid metabolism, nitrogen metabolism and so on[9,38,61]. As an important carbon source for microbial life activities, the synthesis and metabolism of sugars affect the main energy supply[68]. The synthesis and metabolism of lipids mainly affect the formation of cell wall and cell membrane[69]. Therefore, key genes related to gluconeogenesis and lipid metabolism, including *pyk*, *gntK* and *glpK*, were further investigated (Fig. 6).

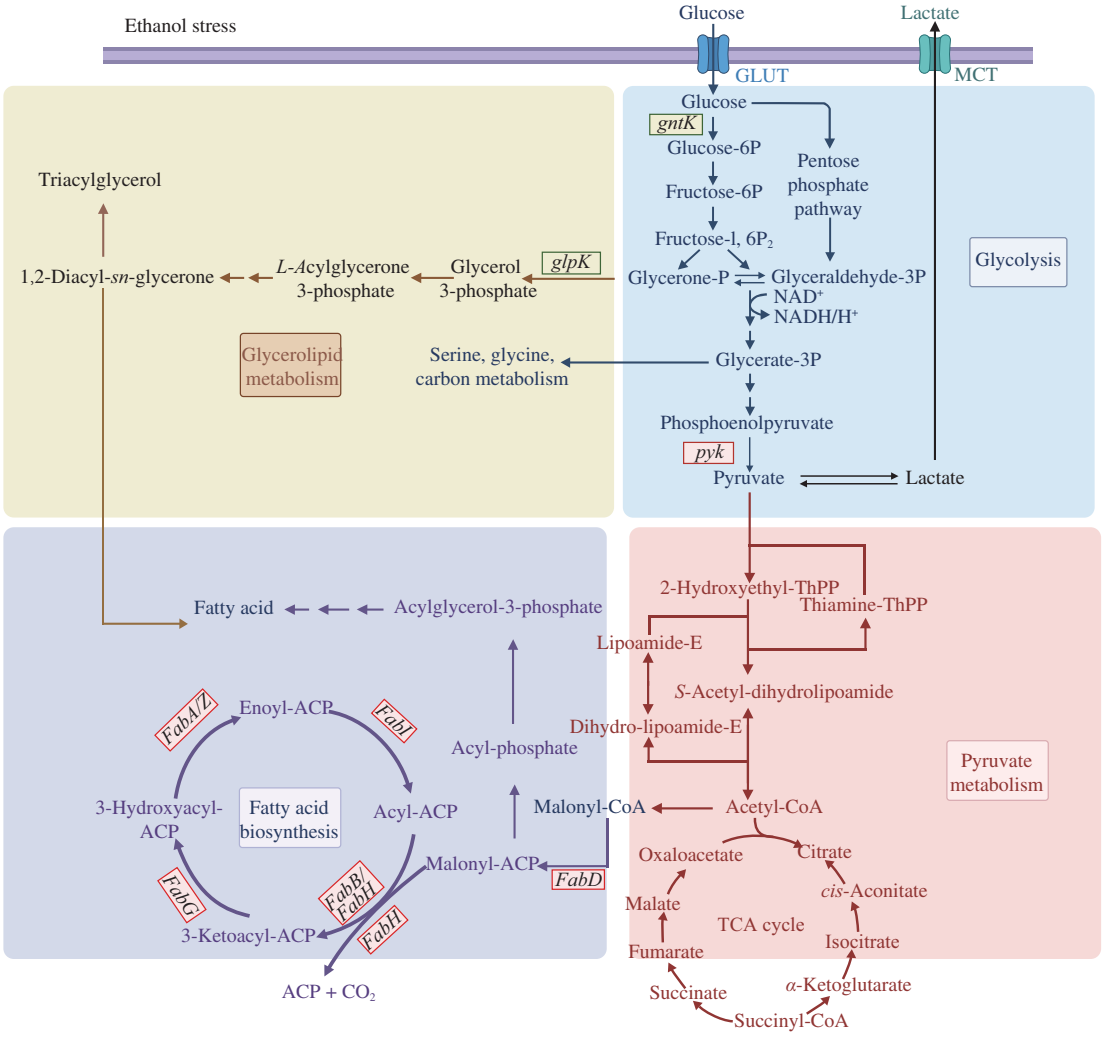

Fig. 6 Key metabolic pathways of *L. hilgardii* Q19 under ethanol stress. The green box represented down-regulated genes and the red box indicated up-regulated genes.

Table 13
Expression of genes related to P-type ATPase.

Gene number	Relative expression	Description of gene function
GQR93_RS09595	1.810 8	Plasma membrane calcium-transporting ATPase
GQR93_RS12990	–0.097 741	Cation-translocating P-type ATPase
GQR93_RS06230	–2.772 3	Cation-transporting P-type ATPase
GQR93_RS01400	–1.976 3	Cadmium-translocating P-type ATPase
GQR93_RS12155	–0.335 77	HAD-IC family P-type ATPase
GQR93_RS07955	–0.009 827 2	Heavy metal translocating P-type ATPase
GQR93_RS05490	–1.853	Copper-translocating P-type ATPase

In PCR amplification of key genes, a single band consistently appears at 1 815, 1 650 and 1 545 bp, aligning precisely with the anticipated size of the target gene (Fig. 7A). Importantly, the primers exhibit a high specificity, avoiding non-specific amplification, and the product concentration is notably robust. These characteristics facilitate efficient cutting and recovery processes. Upon isolating the pNZ8148 plasmid, a single enzyme digestion was performed using the *pstI* restriction endonuclease. Evaluation *via* 10% agarose gel electrophoresis confirms the exceptional quality of the extracted plasmid, showing no signs of degradation and presenting a distinct, solitary band. Post-digestion, we observe a single band at 3 165 bp, a match in size without the emergence of any heterogeneous bands (Fig. 7B). This indicates the plasmid's suitability for cutting and recovery procedures.

L. lactis NZ9000 failed to grow on GM17 plates with chloramphenicol, indicating that *L. lactis* NZ9000 is not resistant to chloramphenicol (Fig. 8). Therefore, the positive clones grown on resistant plates potentially carry the pNZ8148 plasmid. Both the empty plasmid and the target gene-carrying overexpression vector exhibit growth on 5 and 10 g/mL chloramphenicol-resistant GM17 plates. However, their growth ceases on 20 and 50 g/mL chloramphenicol-resistant GM17 plates, indicating an optimal concentration is 10 g/mL.

Subsequently, monoclonal colonies were selected for colony PCR, and colonies with the target bands underwent culture for plasmid extraction. These extracted plasmids were then subject to single digestion using the *pstI* restriction endonuclease. Sequencing of the plasmid from the colony containing 2 target bands of the correct size confirmed the successful introduction of the target gene. Fig. 9A illustrates that the positive clone indeed possesses 2 destination bands post-digestion, aligning with both the plasmid and the target gene's expected sizes.

An analysis of the growth curves (Fig. 10) reveals that the test strain enters the logarithmic growth phase at 1.5 h and stabilizes at 6 h, ultimately reaching a final bacterial growth $OD_{600\ nm}$ of approximately 1.7. Notably, the $OD_{600\ nm}$ at the onset of the logarithmic growth phase is 0.3. As a result, we opted to induce Nisin expression at this juncture. The addition of Nisin for expression induction perturbed the strain's growth pattern when compared to *L. lactis* NZ9000. Although it delayed the onset of the stabilization phase, it had a relatively minor impact on the final growth. This underscores the influence of exogenous plasmid presence on the strain's growth and reproduction dynamics.

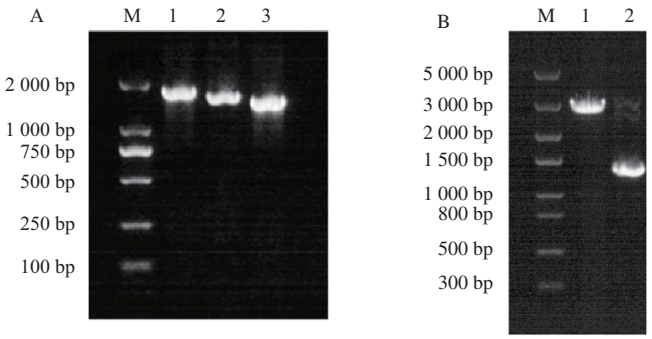

Fig. 7 (A) Full-length amplification of *pyk*, *gntK* and *glpK*. M: DL 2000 marker; lane 1: *glpK* (1 815 bp); lane 2: *gntK* (1 650 bp); lane 3: *pyk* (1 545 bp). (B) Plasmid pNZ8148 *pstI* single enzyme digestion. M: DL 5000 Marker; lane 1: pNZ8148 single enzyme fragment digestion; lane 2: pNZ8148 plasmid.

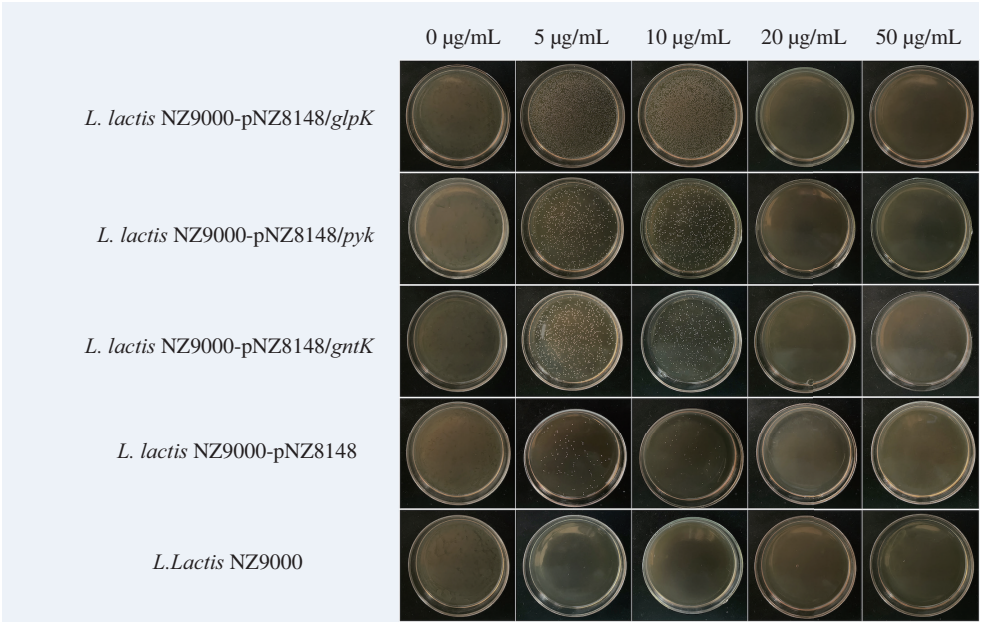

Fig. 8 Plate of positive clone strain.

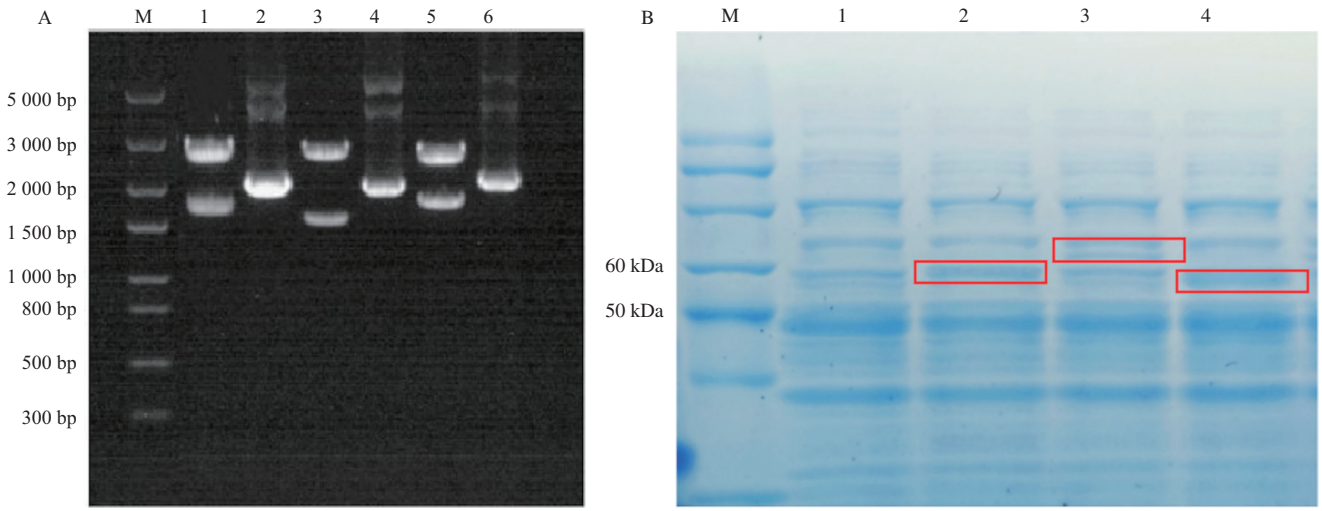

Fig. 9 (A) *PstI* single enzyme digestion gel electrophoresis. M: DL5K Marker; lane 1: pNZ8148/*gntK* enzyme cut bands; lane 2: pNZ8148/*gntK* strip without enzyme digestion; lane 3: pNZ8148/*glpK* enzyme cut bands; lane 4: pNZ8148/*glpK* strip without enzyme digestion; lane 5: pNZ8148/*pyk* enzyme cut bands; lane 6: pNZ8148/*pyk* uncut bands. (B) SDS-PAGE expression analysis of *glpK*, *pyk* and *gntK* genes overexpressed in *L. lactis* NZ9000. M: protein standard marker; lane 1: *L. lactis* NZ9000-pNZ8148; lane 2: *L. lactis* NZ9000-pNZ8148/*gntK*; lane 3: *L. lactis* NZ9000-pNZ8148/*pyk*; lane 4: *L. lactis* NZ9000-pNZ8148/*glpK*.

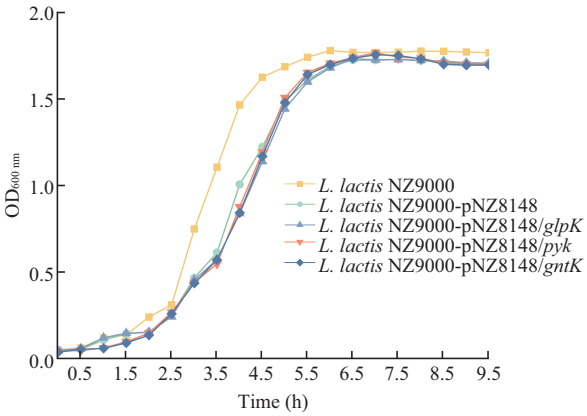

Fig. 10 Growth curve of *L. lactis* NZ9000 induced expression.

The target gene's induction *via* Nisin for 3 h culminated in SDS-PAGE. Fig. 9B exhibits discernible bands of expressed target proteins at relative molecular weights of 61, 64, and 57 kDa, aligning precisely with the anticipated sizes.

Under stress conditions, glucokinase utilizes a proton gradient to phosphorylate glucose in the medium, thereby providing energy for substance transport[70]. This enables cells to maintain normal growth and metabolic activities even under stressful conditions. The gntRKU operon encoding part of the GntI system involved in gluconate uptake and catabolism. Specifically, the operon was shown to encode gluconate kinase[71]. *L. lactis* NZ9000-pNZ8148/*gntK* exhibited significantly lower viable bacterial counts in the presence of low concentrations of ethanol (4%, 8%, 10% (*V*/*V*)) compared to the control strain, *L. lactis* NZ9000-pNZ8148, when cultured in GM17 medium. Specifically, the reduction in viable counts was measured at 37.17%, 10.55%, and 25.55% for the respective ethanol concentrations. In contrast, under relatively high ethanol content conditions (12%, 14% (*V*/*V*)), the viable counts for *L. lactis* NZ9000-pNZ8148/*gntK* increased by 6.54% and 22.78%.

For LAB, the primary source of energy is linked to the glycolytic pathway. Pyruvate kinase, an essential glycolytic enzyme, acts as a central switch for carbon flux distribution[72]. The activities of glycolytic enzyme (including phosphofructokinase, pyruvate kinase and lactate dehydrogenase) are both elevated in LAB after stress[73]. *pyk* genes, encoding pyruvate kinases, is associated with stress tolerance in LAB. For example, under acid stress conditions (pH 4.0), the *pyk* high-yielding strain exhibited a remarkable 45-fold increase in survival compared to the control. Furthermore, catabolism control protein A (CcpA) positively regulated *pyk* transcription[74]. Similarly, *L. lactis* NZ9000-pNZ8148/*pyk*, when cultivated in GM17 medium, displayed distinct responses to ethanol stress. In the presence of 4% and 8% (*V*/*V*) ethanol content, viable counts increased by 13.18% and 22.94%, respectively. However, at higher ethanol concentrations (10%, 12%, and 14% (*V*/*V*)), viable counts decreased by 8.62%, 12.56%, and 19.96%.

Glycerol kinase encoded by *glpK* plays a crucial role in glycerol utilization by catalyzing the transfer of phosphate from ATP to glycerol, yielding 3-phosphoglycerol—an essential intermediate in energy metabolism and glycerolipid production[75]. No significant variation in viable counts was observed for *L. lactis* NZ9000-pNZ8148/*glpK* under 4% (*V*/*V*) ethanol stress. However, at 8% and 10% (*V*/*V*) ethanol content in GM17 medium, viable bacterial counts decreased by 10.32% and 6.26%, respectively. In contrast, under 12% and 14% (*V*/*V*) ethanol conditions, viable bacterial counts increased significantly, by 47.94% and 54.43%.

In summary, these results suggest a positive influence of the *pyk* gene on strain survival at lower ethanol concentrations (4%, 8% (*V*/*V*)), while the *gntK* and *glpK* genes positively impact strain survival at higher ethanol concentrations (12%, 14% (*V*/*V*)) (Fig. 11). The reason for this phenomenon may be due to differences in the expression of heterologous and homologous proteins in the host strain[76]. For example, it has been shown that overexpression of recombinant proteins in *E. coli* triggers a metabolic stress response, leading to a dramatic decrease in growth and product formation after induction[77]. Meanwhile, overexpression of *recT* in *L. lactis* NZ9000 and *E. coli* BL21 indicated that the expression of the antacid component resulted in metabolic loading of the recombinant strains, thus affecting their growth[78].

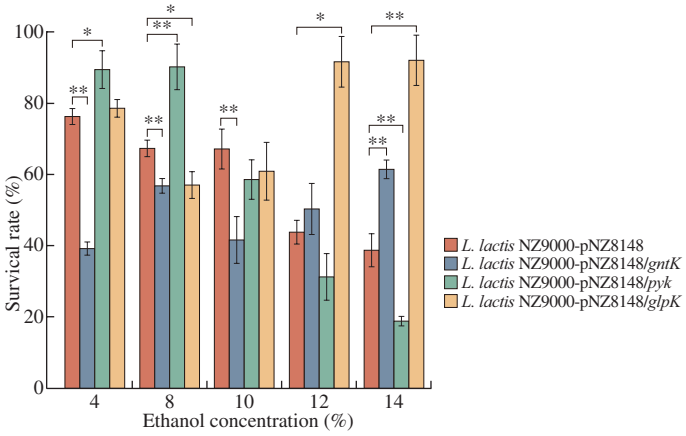

Fig. 11 Survival rate of overexpressed strains under ethanol stress. $^{*}P < 0.05$, $^{**}P < 0.01$.

4. Conclusion

Global warming has led to an increase in the concentration of ethanol in wine, making malolactic fermentation more difficult. Interestingly, *L. hilgardii* Q19 can maintain a high survival rate and perform well in harsh environments where most malolactic bacteria cannot survive. In this work, we characterised the physiological changes of *L. hilgardii* Q19 under 19% (*V*/*V*) ethanol stress for the first time and unravelled the molecular mechanisms of *L. hilgardii* Q19 in response to ethanol stress combined with transcriptomics.

Physical and chemical indicators analysis data showed that *L. hilgardii* Q19 combated ethanol stress by increasing the energy metabolism, taking up more glutathione, inhibiting ATPase activity and reducing cell membrane fluidity. In transcriptomic analyses, genes in the pyruvate metabolism and glutathione metabolism pathways were up-regulated. Conversely, genes in the ABC transporter protein pathway and phosphotransferase system were significantly down-regulated. These results were consistent with the physicochemical analysis data. In summary, *gntK*, *pyk* and *glpK*, which are related to sugar metabolism, were screened as key genes in *L. hilgardii* Q19 against ethanol stress and their functions were verified by heterologous overexpression. The functions of key genes were further evaluated under different ethanol concentrations. The results indicated that pyruvate kinase had a positive effect on strain survival under low ethanol stress conditions, while glucokinase and glycerol kinase were the main factors under high ethanol stress conditions. These findings could help to understand the resistance mechanisms of *L. hilgardii* to ethanol stress.

Conflict of interest

The authors have declared that no conflict of interest exists.

Acknowledgements

This work was financially supported by the National Natural Science Foundation of China (32160578) and Natural Science Foundation of Ningxia Hui Autonomous Region (2025AAC020032).

References

[1] G. Gutiérrez-Gamboa, W. Zheng, F. Martínez de Toda, Current viticultural techniques to mitigate the effects of global warming on grape and wine quality: a comprehensive review, Food Res. Int. 139 (2021) 109946. https://doi.org/10.1016/j.foodres.2020.109946.

[2] G.V. Jones, L.B. Webb, Climate change, viticulture, and wine: challenges and opportunities, J. Wine Res. 21 (2010) 103-106. https://doi.org/10.1080/09571264.2010.530091.

[3] S. Dequin, J.L. Escudier, M. Bely, et al., How to adapt winemaking practices to modified grape composition under climate change conditions, OENO One 51 (2017) 205-214. https://doi.org/10.20870/oeno-one.2017.51.2.1584.

[4] B.M. Bravo-Ferrada, A. Gómez-Zavaglia, L. Semorile, et al., Effect of the fatty acid composition of acclimated oenological *Lactobacillus plantarum* on the resistance to ethanol, Lett. Appl. Microbiol. 60 (2015) 155-161. https://doi.org/10.1111/lam.12350.

[5] N. Haddaji, A.K. Mahdhi, M.B. Ismaiil, et al., Effect of environmental stress on cell surface and membrane fatty acids of *Lactobacillus plantarum*, Arch. Microbiol. 199 (2017) 1243–1250. https://doi.org/10.1007/s00203-017-1395-9.

[6] K. Gustaw, P. Koper, M. Polak-Berecka, et al., Genome and pangenome analysis of *Lactobacillus hilgardii* FLUB—a new strain isolated from mead, Int. J. Mol. Sci. 22 (2017) 3780. https://doi.org/10.3390/ijms22073780.

[7] D.E. Zhuravleva, Z.I. Iskhakova, G.D. Ozhegov, et al., Complete genome sequence of *Lactobacillus hilgardii* LMG 7934 carrying the gene encoding for the novel PII-like protein PotN, Curr. Microbiol. 77 (2020) 3538-3545. https://doi.org/10.1007/s00284-020-02161-6.

[8] L. Wang, G. Huang, W. Ma, et al., Preparation and application of directed vat set indigenous freeze-drying *Lentilactobacillus hilgardii* Q19 starter in winemaking, Foods 12 (2023) 1053. https://doi.org/10.3390/foods12051053.

[9] Y. Cheng, Study on the mechanism of ethanol tolerance in *Arthrobacter simplex* based on the analysis of cell membrane lipid composition, Tianjin Univ. Sci. Technol., Tianjin, China, 2013. (In Chinese).

[10] M.G. Silveira, M.V.S. Romão, M.C. Loureiro-Dias, et al., Flow cytometric assessment of membrane integrity of ethanol-stressed *Oenococcus oeni* cells, Appl. Environ. Microbiol. 68 (2002) 6087-6093. https://doi.org/10.1128/aem.68.12.6087-6093.2002.

[11] J.P. Morth, B.P. Pedersen, M.J. Buch-Pedersen, et al., A structural overview of the plasma membrane Na^+,K^+-ATPase and H^+-ATPase ion pumps, Nat. Rev. Mol. Cell Biol. 12 (2011) 60-70. https://doi.org/10.1038/nrm3031.

[12] C. Wu, J. Zhang, M. Wang, et al., *Lactobacillus casei* combats acid stress by maintaining cell membrane functionality, J. Ind. Microbiol. Biotechnol. 39 (2012) 1031-1039. https://doi.org/10.1007/s10295-012-1104-2.

[13] H. Zhang, B. Kong, H. Liu, et al., Physiology and antioxidant activity of *Pediococcus pentosaceus* R1 and *Lactobacillus fermentum* R6 in response to lactic acid stress, LWT-Food Sci. Technol. 149 (2021) 111878. https://doi.org/10.1016/j.lwt.2021.111878.

[14] T. Zhang, Y. Guo, X. Fan, et al., Protection mechanism of metal ion pre-stress on *Lactobacillus acidophilus* CICC 6074 under acid tolerance, J. Agric. Food Chem. 71 (2023) 13304-13315. https://doi.org/10.1021/acs.jafc.3c01970.

[15] A.S. Pivovarov, F. Calahorro, R.J. Walker, Na^+/K^+-pump and neurotransmitter membrane receptors, Invertebr. Neurosci. 19 (2019) 1. https://doi.org/10.1007/s10158-018-0221-7.

[16] F. Zuo, R. Yu, X. Feng, et al., Combination of heterogeneous catalase and superoxide dismutase protects *Bifidobacterium longum* strain NCC2705 from oxidative stress, Appl. Microbiol. Biotechnol. 98 (2014) 7523-7534. https://doi.org/10.1007/s00253-014-5851-z.

[17] M. Serata, E. Yasuda, T. Sako, Effect of superoxide dismutase and manganese on superoxide tolerance in *Lactobacillus casei* strain Shirota and analysis of multiple manganese transporters, Biosci. Microbiota Food Health 37 (2018) 31-38. https://doi.org/10.12938/bmfh.17-018.

[18] T. Wang, Z. Xu, S. Lu, et al., Effects of glutathione on acid stress resistance and symbiosis between *Streptococcus thermophilus* and *Lactobacillus delbrueckii* subsp. *bulgaricus*, Int. Dairy J. 61 (2016) 22-28. https://doi.org/10.1016/j.idairyj.2016.03.012.

[19] F. Tao, W. Jing, Oxidative stress tolerance and antioxidant capacity of lactic acid bacteria as probiotic: a systematic review, Gut Microbes 12 (2020) e1801944. https://doi.org/10.1080/19490976.2020.1801944.

[20] T.H. Nguyen, J.S. Kim, H.J. Kwon, et al., The effect of a glutathione (GSH)-containing cryo-protectant on the viability of probiotic cells using a freeze-drying process, Fermentation 9 (2023) 187. https://doi.org/10.3390/fermentation9020187.

[21] M.G. Silveira, M. Baumgärtner, F.M. Rombouts, et al., Effect of adaptation to ethanol on cytoplasmic and membrane protein profiles of *Oenococcus oeni*, Appl. Environ. Microbiol. 70 (2004) 2748-2755. https://doi.org/10.1128/AEM.70.5.2748-2755.2004.

[22] A. Surya, X. Liu, M.J. Miller, Glutathione utilization in *Lactobacillus fermentum* CECT 5716, J. Agric. Food Chem. 66 (2018) 12651-12656. 12651-12656. https://doi.org/10.1021/acs.jafc.8b06136.

[23] M. Margalef-Català, I. Araque, S. Weidmann, et al., Protective role of glutathione addition against wine-related stress in *Oenococcus oeni*, Food Res. Int. 90 (2016) 8-15. https://doi.org/10.1016/j.foodres.2016.10.006.

[24] L. Guo, H. Wang, M. Li, et al., Quantification of reduced and oxidized glutathione in wine by MALDI-TOF MS, J. Food Compos. Anal. 115 (2022) 104956. https://doi.org/10.1016/j.jfca.2022.104956.

[25] B. Castro, M. Citterico, S. Kimura, et al., Stress-induced reactive oxygen species compartmentalization, perception and signalling, Nat. Plants. 7 (2021) 403-412. https://doi.org/10.1038/s41477-021-00887-0.

[26] J. Yang, J. Luo, X. Tian, et al., Progress in understanding oxidative stress, aging, and aging-related diseases, Antioxidants 13 (2024) 394. https://doi.org/10.3390/antiox13040394.

[27] X. Chen, Z. Zhong, Z. Xu, et al., 2',7'-dichlorodihydrofluorescein as a fluorescent probe for reactive oxygen species measurement: forty years of application and controversy, Free Radic. Res. 44 (2010) 587-604. https://doi.org/10.3109/10715761003709802.

[28] T. Liu, L. Sun, Y. Zhang, et al., Imbalanced GSH/ROS and sequential cell death, J. Biochem. Mol. Toxicol. 36 (2022) e22942. https://doi.org/10.1002/jbt.22942.

[29] S. Chu-Ky, R. Tourdot-Marechal, P.A. Marechal, et al., Combined cold, acid, ethanol shocks in *Oenococcus oeni*: effects on membrane fluidity and cell viability, Biochim. Biophys. Acta. 1717 (2005) 118-124. https://doi.org/10.1016/j.bbamem.2005.09.015.

[30] V. Capozzi, D. Fiocco, G. Spano, Responses of lactic acid bacteria to cold stress, in: E. Tsakalidou, K. Papadimitriou (Eds.), Stress responses of lactic acid bacteria to cold stress, Springer, Boston, 2011, pp. 91-110. https://doi.org/10.1007/978-0-387-92771-8_5.

[31] C. Wu, J. Zhang, W. Chen, et al., A combined physiological and proteomic approach to reveal lactic-acid-induced alterations in *Lactobacillus casei* Zhang and its mutant with enhanced lactic acid tolerance, Appl. Microbiol. Biotechnol. 93 (2012) 707-722. https://doi.org/10.1007/s00253-011-3757-6.

[32] J. Meneghel, S. Passot, S. Cenard, et al., Subcellular membrane fluidity of *Lactobacillus delbrueckii* subsp. *bulgaricus* under cold and osmotic stress, Appl. Microbiol. Biotechnol. 101 (2017) 6907-6917. https://doi.org/10.1007/s00253-017-8444-9.

[33] A. Bodzen, A. Jossier, S. Dupont, et al., Increased survival of *Lactococcus lactis* strains subjected to freeze-drying after cultivation in an acid medium: involvement of membrane fluidity cultivation in acid medium to improve bacterial survival of freeze-drying, Food Technol. Biotechnol. 59 (2021) 443-453. https://doi.org/10.17113/ftb.59.04.21.7076.

[34] Y. Yoon, H. Lee, S. Lee, et al., Membrane fluidity-related adaptive response mechanisms of foodborne bacterial pathogens under environmental stresses, Food Res. Int. 72 (2015) 25-36. https://doi.org/10.1016/j.foodres.2015.03.016.

[35] Y. Qi, H. Liu, X. Chen, et al., Engineering microbial membranes to increase stress tolerance of industrial strains, Metab. Eng. 53 (2019) 24-34. https://doi.org/10.1016/j.ymben.2018.12.010.

[36] M. Rosenberg, N.F. Azevedo, A. Ivask, Propidium iodide staining underestimates viability of adherent bacterial cells, Sci. Rep. 9 (2019) 6483. https://doi.org/10.1038/s41598-019-42906-3.

[37] Y.P. Khasa, S. Mohanty, Growth physiology and kinetics, in: Fundamentals of bacterial physiology and metabolism, Springer, Singapore, 2021. https://doi.org/10.1007/978-981-16-0723-3_5.

[38] S. Yao, R. Zhou, Y. Jin, et al., Formation of biofilm changed the responses of *Tetragenococcus halophilus* to ethanol stress revealed by transcriptomic and proteomic analyses, Food Res. Int. 161 (2022) 111817. https://doi.org/10.1016/j.foodres.2022.111817.

[39] A.A. Akhtar, D.P.J. Turner, The role of bacterial ATP-binding cassette (ABC) transporters in pathogenesis and virulence: therapeutic and vaccine potential, Microb. Pathog. 171 (2022) 105734. https://doi.org/10.1016/j.micpath.2022.105734.

[40] J.P. Bourdineaud, B. Nehmé, S. Tesse, et al., A bacterial gene homologous to ABC transporters protects *Oenococcus oeni* from ethanol and other stress factors in wine, Int. J. Food Microbiol. 92 (2004) 1-14. https://doi.org/10.1016/S0168-1605(03)00162-4.

[41] I.C. Duru, A. Ylinen, S. Belanov, et al., Transcriptomic time-series analysis of cold- and heat-shock response in psychrotrophic lactic acid bacteria, BMC Genomics 22 (2021) 28. https://doi.org/10.1186/s12864-020-07338-8.

[42] M. Li, Q. Wang, X. Song, et al., iTRAQ-based proteomic analysis of responses of *Lactobacillus plantarum* FS5-5 to salt tolerance, Ann. Microbiol. 69 (2019) 377-389. https://doi.org/10.1007/s13213-018-1425-0.

[43] M. Liu, X. Zeng, Y. He, et al., iTRAQ-based quantitative proteomic analysis of the effect of heat shock on freeze-drying of *Lactobacillus acidophilus* ATCC4356, J. Proteomics 56 (2021) 5569-5580. https://doi.org/10.1111/are.14880.

[44] Z. Zhu, P. Yang, J. Yang, et al., Comparative transcriptome analysis reveals the contribution of membrane transporters to acid tolerance in *Lactococcus lactis*, J. Biotechnol. 357 (2022) 9-17. https://doi.org/10.1016/j.jbiotec.2022.08.006.

[45] M. Braibant, P. Lefèvre, L. de Wit, et al., A *Mycobacterium tuberculosis* gene cluster encoding proteins of a phosphate transporter homologous to the *Escherichia coli* Pst system, Gene 176 (1996) 171-176. https://doi.org/10.1016/0378-1119(96)00242-9.

[46] D. Gonzalez, M. Richez, C. Bergonzi, et al., Crystal structure of the phosphate-binding protein (PBP-1) of an ABC-type phosphate transporter from *Clostridium perfringens*, Sci. Rep. 4 (2014) 6636. https://doi.org/10.1038/srep06636.

[47] D. Rees, E. Johnson, O. Lewinson, ABC transporters: the power to change, Nat. Rev. Mol. Cell Biol. 10 (2009) 218-227. https://doi.org/10.1038/nrm2646.

[48] M. Yang, T. Mu, W. Zhong, et al., Analysis of gluconate metabolism for pyruvate production in engineered *Escherichia coli* based on genome-wide transcriptomes, Lett. Appl. Microbiol. 65 (2017) 165-172. https://doi.org/10.1111/lam.12758.

[49] A. Stincone, A. Prigione, T. Cramer, et al., The return of metabolism: biochemistry and physiology of the pentose phosphate pathway, Biol. Rev. Camb. Philos. Soc. 90 (2015) 927-963. https://doi.org/10.1111/brv.12140.

[50] J. Chen, H. Wu, W. Zhang, et al., Ribose-5-phosphate isomerases: characteristics, structural features, and applications, Appl. Microbiol. Biotechnol. 104 (2020) 6429-6441. https://doi.org/10.1007/s00253-020-10735-4.

[51] Y. Xie, J. Li, Y. Ding, et al., An atlas of bacterial two-component systems reveals function and plasticity in signal transduction, Cell Rep. 41 (2022) 111502. https://doi.org/10.1016/j.celrep.2022.111502.

[52] A. Pöntinen, M. Lindström, M. Skurnik, et al., Screening of the two-component-system histidine kinases of *Listeria monocytogenes* EGD-e: LiaS is needed for growth under heat, acid, alkali, osmotic, ethanol and oxidative stresses, Food Microbiol. 65 (2017) 36-43. https://doi.org/10.1016/j.fm.2017.01.018.

[53] G. Li, Morigen, Y. Yao, TorR/TorS two-component system resists extreme acid environment by regulating the key response factor RpoS in *Escherichia coli*, Gene 821 (2022) 146295. https://doi.org/10.1016/j.gene.2022.146295.

[54] G. Tang, S. Wang, D. Lu, et al., Two-component regulatory system ActS/ActR is required for *Sinorhizobium meliloti* adaptation to oxidative stress, Microbiol. Res. 198 (2017) 1-7. https://doi.org/10.1016/j.micres.2017.01.005.

[55] Y. Cui, M. Wang, Y. Zheng, et al., The carbohydrate metabolism of *Lactiplantibacillus plantarum*, Int. J. Mol. Sci. 22 (2021) 13452. https://doi.org/10.3390/ijms222413452.

[56] X. Pang, C. Liu, P. Lyu, et al., Identification of quorum sensing signal molecule of *Lactobacillus delbrueckii subsp. bulgaricus*, J. Agric. Food Chem. 64 (2016) 9421-9427. https://doi.org/10.1021/acs.jafc.6b04016.

[57] W. Yin, Y. Wang, L. Liu, et al., Biofilms: the microbial "protective clothing" in extreme environments, Int. J. Mol. Sci. 20 (2019) 3423. https://doi.org/10.3390/ijms20143423.

[58] Y. Wang, Z. Bian, Y. Wang, Biofilm formation and inhibition mediated by bacterial quorum sensing, Appl. Microbiol. Biotechnol. 106 (2022) 6365-6381. https://doi.org/10.1016/j.micres.2023.127414.

[59] G. Vrancken, T. Rimaux, S. Weckx, et al., Environmental pH determines citrulline and ornithine release through the arginine deiminase pathway in

Lactobacillus fermentum IMDO 130101, Int. J. Food Microbiol. 135 (2009) 216-222. https://doi.org/10.1016/j.ijfoodmicro.2009.07.035.

[60] G. Vrancken, T. Rimaux, D. Wouters, et al., The arginine deiminase pathway of *Lactobacillus fermentum* IMDO 130101 responds to growth under stress conditions of both temperature and salt, Food Microbiol. 26 (2009) 720-727. https://doi.org/10.1016/j.fm.2009.07.006.

[61] L. Díez, A. Solopova, R. Fernández-Pérez, et al., Transcriptome analysis shows activation of the arginine deiminase pathway in *Lactococcus lactis* as a response to ethanol stress, Int. J. Food Microbiol. 257 (2017) 41-48. https://doi.org/10.1016/j.ijfoodmicro.2017.05.017.

[62] T. Pols, S. Singh, C. Deelman-Driessen, et al., Enzymology of the pathway for ATP production by arginine breakdown, FEBS J. 288 (2021) 293-309. https://doi.org/10.1111/febs.15337.

[63] M.E. Arena, M.C. Manca de Nadra, R. Muñoz, The arginine deiminase pathway in the wine lactic acid bacterium *Lactobacillus hilgardii* X1B: structural and functional study of the arcABC genes, Gene 301 (2002) 61-66. https://doi.org/10.1016/s0378-1119(02)01083-1.

[64] K. Veeravalli, D. Boyd, B.L. Iverson, et al., Laboratory evolution of glutathione biosynthesis reveals natural compensatory pathways, Nat. Chem. Biol. 7 (2011) 101-105. https://doi.org/10.1038/nchembio.499

[65] S.D. Pophaly, P. Singh, S.D. Pophaly, et al., Glutathione biosynthesis and activity of dependent enzymes in food-grade lactic acid bacteria harbouring multidomain bifunctional fusion gene (*gshF*), J. Appl. Microbiol. 123 (2017) 194-203. https://doi.org/10.1111/jam.13471.

[66] W.J. Israelsen, M.G. Vander Heiden, Pyruvate kinase: function, regulation and role in cancer, Semin. Cell Dev. Biol. 43 (2015) 43-51. https://doi.org/10.1016/j.semcdb.2015.08.004.

[67] J. Da, M. Xi, M. Liu, et al., Transcriptome analysis and functional gene identification reveals potential mechanisms of heat stress response of *Lactiplantibacillus plantarum* CGMCC8198, Food Biosci. 51 (2023) 102202. https://doi.org/10.1016/j.fbio.2022.102202.

[68] H.J. Fromm, M.S. Hargrove, Carbohydrate metabolism A: glycolysis and gluconeogenesis, in: Essentials of biochemistry, Springer, Berlin, Heidelberg, 2012. https://doi.org/10.1007/978-3-642-19624-9_8.

[69] G.F. Grabner, H. Xie, M. Schweiger, et al., Lipolysis: cellular mechanisms for lipid mobilization from fat stores, Nat. Metab. 3 (2021) 1445-1465. https://doi.org/10.1038/s42255-021-00493-6.

[70] J. Stülke, W. Hillen, Regulation of carbon catabolism in *Bacillus* species, Annu. Rev. Microbiol. 54 (2000) 849-880. https://doi.org/10.1146/annurev.micro.54.1.849.

[71] H. Izu, O. Adachi, M. Yamada, Gene organization and transcriptional regulation of the *gntRKU* operon involved in gluconate uptake and catabolism of *Escherichia coli*, J. Mol. Biol. 267 (1997) 778-793. https://doi.org/10.1006/jmbi.1996.0913.

[72] N. Schormann, K.L. Hayden, P. Lee, et al., An overview of structure, function, and regulation of pyruvate kinases, Protein Sci. 28 (2019) 1771-1784. https://doi.org/10.1002/pro.3691.

[73] C. Li, J. Sun, X. Qi, et al., NaCl stress impact on the key enzymes in glycolysis from *Lactobacillus bulgaricus* during freeze-drying, Braz. J. Microbiol. 46 (2015) 1193-1199. https://doi.org/10.1590/S1517-838246420140595

[74] L.G. Monahan, I.V. Hajduk, S.P. Blaber, et al., Coordinating bacterial cell division with nutrient availability: a role for glycolysis, mBio 5 (2014) e00935-14. https://doi.org/10.1128/mBio.00935-14.

[75] R. Sivaramakrishnan, A. Incharoensakdi, Enhancement of lipid production in *Synechocystis* spp. PCC 6803 overexpressing glycerol kinase under oxidative stress with glycerol supplementation, Bioresour. Technol. 267 (2018) 532-540. https://doi.org/10.1016/j.biortech.2018.07.058.

[76] C. Gustafsson, S. Govindarajan, J. Minshull, Codon bias and heterologous protein expression, Trends Biotechnol. 22 (2004) 346-353. https://doi.org/10.1016/j.tibtech.2004.04.006.

[77] A.B. Singh, K.J. Mukherjee, Supplementation of substrate uptake gene enhances the expression of *rhIFN-β* in high cell density fed-batch cultures of *Escherichia coli*, Mol. Biotechnol. 54 (2013) 692-702. https://doi.org/10.1007/s12033-012-9611-y.

[78] Z. Zhu, X. Ji, Z. Wu, et al., Improved acid-stress tolerance of Lactococcus lactis NZ9000 and Escherichia coli BL21 by overexpression of the anti-acid component *RecT*, Ind. Microbiol. Biotechnol. 45 (2018) 1091-1101. https://doi.org/10.1007/s10295-018-2075-8.